Electronic Supplementary Information for

Visible Chemosensor Based on Carbohydrazide for Fe(II), Co(II) and Cu(II) in Aqueous Solution

Minuk Yang,[a] Ju Byeong Chae,[a] Cheal Kim,[a]* Roger G. Harrison[b]*

[a] *Department of Fine Chemistry and Department of Interdisciplinary Bio IT Materials, Seoul National University of Science and Technology, Seoul 139-743, Korea. Fax: +82-2-973-9149; Tel: +82-2-970-6693; E-mail: chealkim@seoultech.ac.kr.*

[b] *Department of Chemistry and Biochemistry, Brigham Young University, Provo, UT, 84602. Fax: 1-801-422-0153; Tel: 1-801-422-8096; E-mail: roger_harrison@byu.edu.*

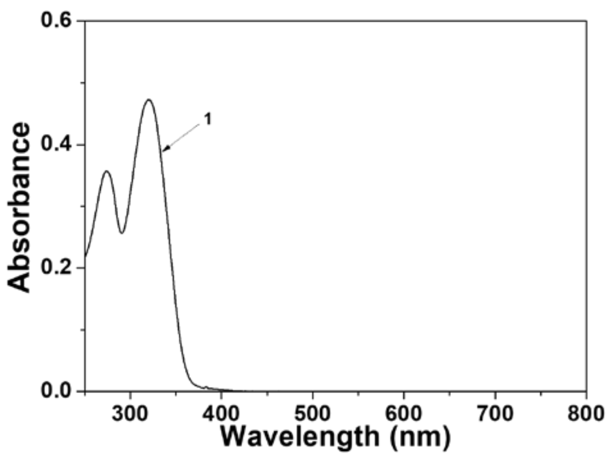

Figure S1. UV-vis spectrum of sensor (30 μM).

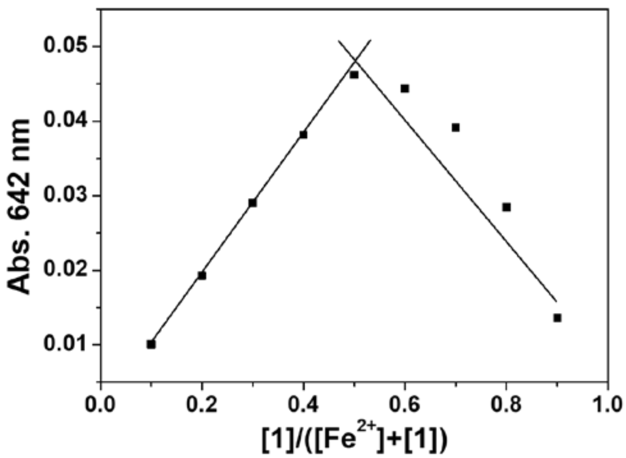

Figure S2. Job plot for the binding of **1** with Fe^{2+}. Absorbance at 642 nm was plotted as a functio n of the molar ratio [**1**]/([**1**] + [Fe^{2+}]). The total concentration of ferrous ion with sensor **1** was 3. 0 x 10^{-5} M.

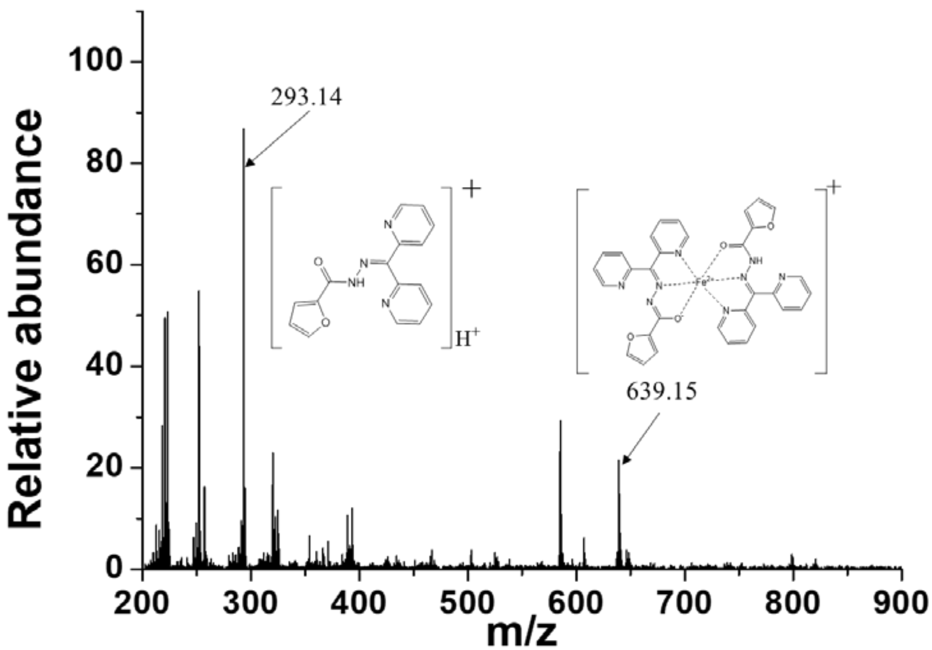

Figure S3. Mass spectroscopy data for Fe(II) plus sensor.

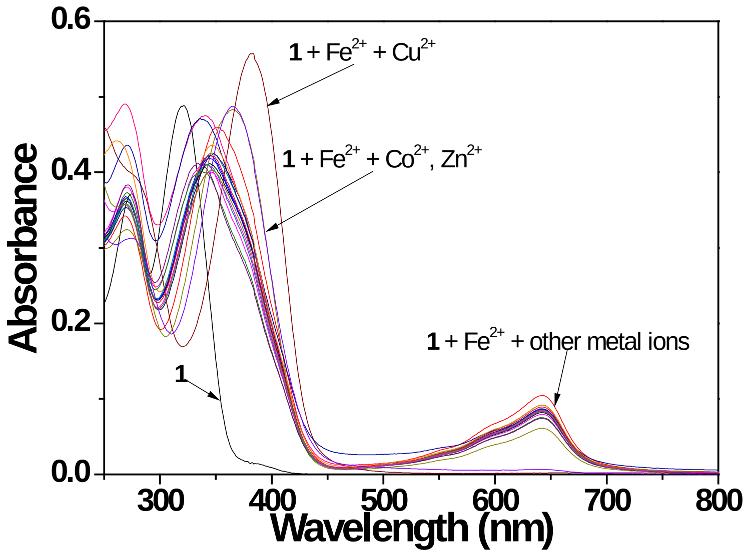

Figure S4. Uv-vis absorption of sensor (1) in the presence of Fe(II) and other metal ions. Conditions: aqueous solution of 30 μM sensor and 1.0 equivalent of Fe(II) and 1.0 equivalent of other metal ion in bis-tris buffer (10 mM) at pH 7.0.

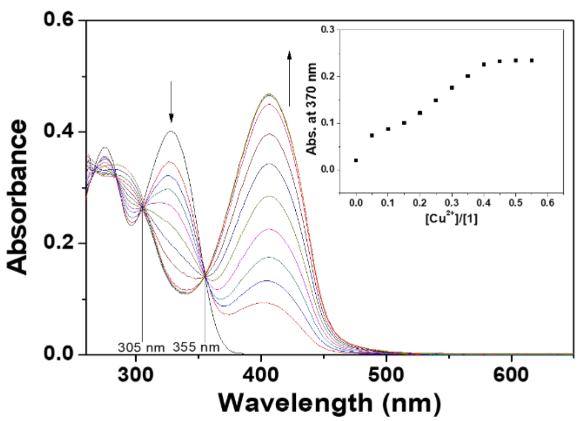

Figure S5. Absorption spectral changes of **1** (30 μM) after addition of increasing amounts of Cu^{2+} in buffer (bis-tris 10 mM, pH 7.0). Inset: Absorption at 370 nm versus the number of equiv of Cu^{2+} added.

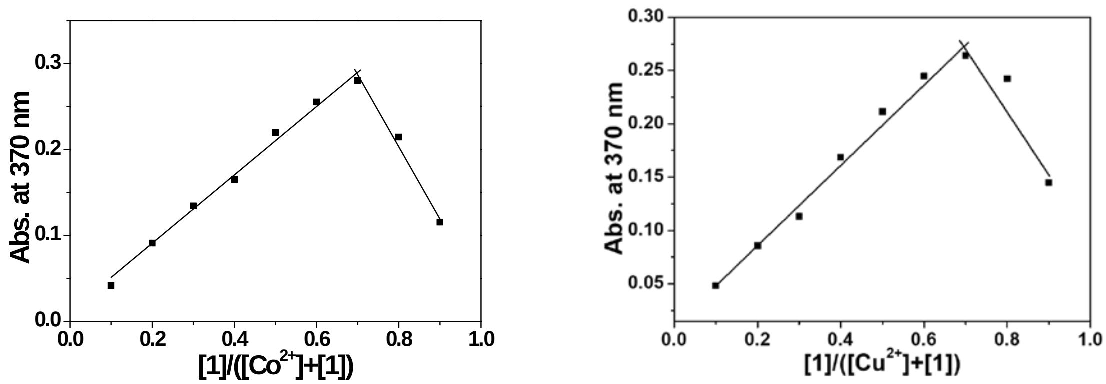

Figure S6. Job plots for the binding of **1** with Co^{2+} and Cu^{2+}. Absorbance at 370 nm was plotted as a function of the molar ratio [**1**]/([**1**] + [M^{2+}]). The total concentration of cobalt or cupper ion with sensor **1** was 3.0 x 10^{-5} M.

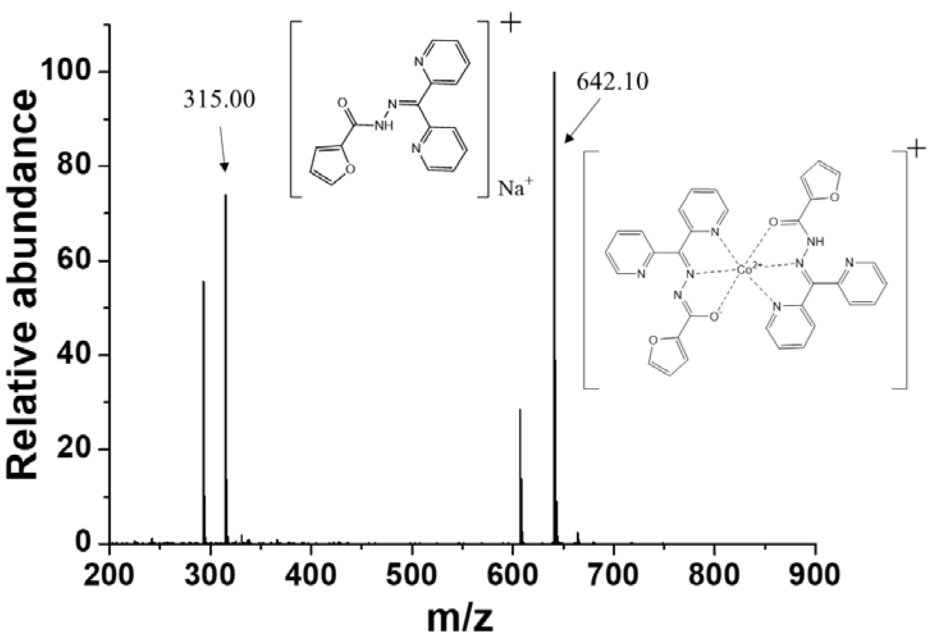

Figure S7. Mass spectrum for Co(II) plus sensor.

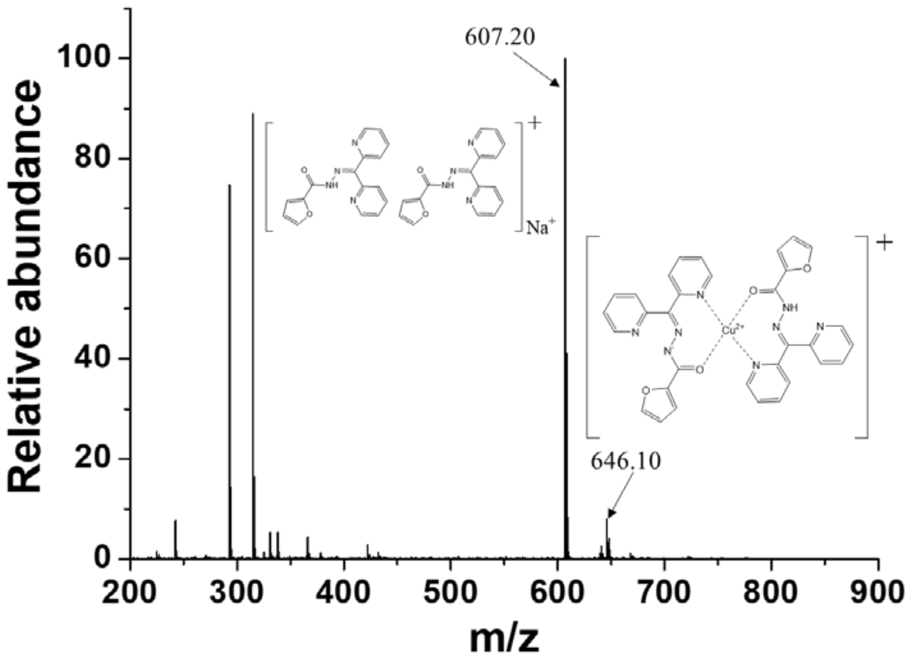

Figure S8. Mass spectrum for Cu(II) plus sensor.

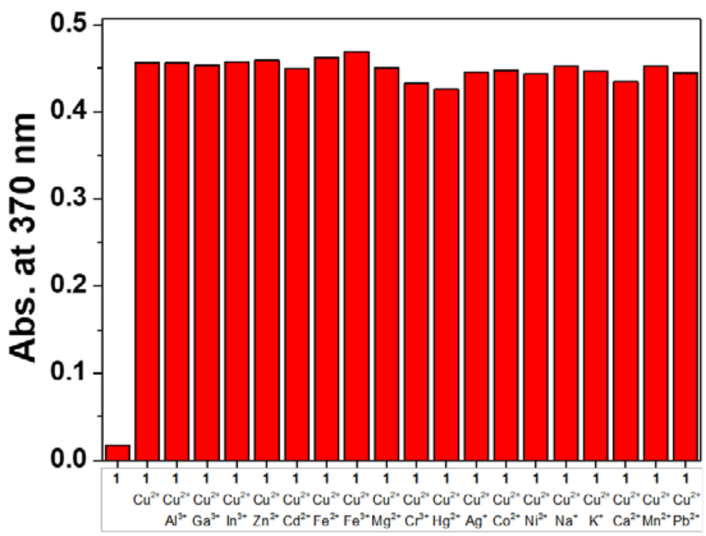

Figure S9. Absorption spectral changes of **1** and Cu^{2+} (30 μM) in the absence and presence of 0.5 equiv of different metal ions in buffer (bis-tris 10 mM, pH 7.0).

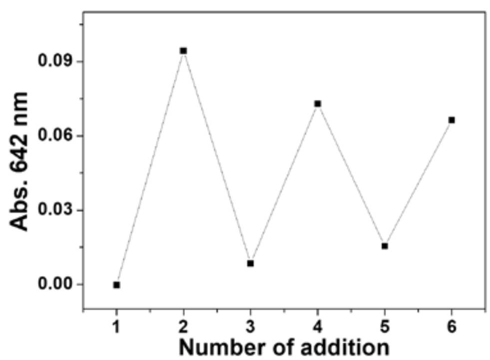

a)

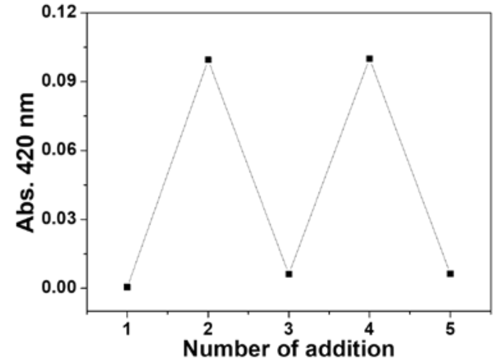

b)

Figure S10. Reusability of sensor with Fe(II) (a) and Co(II) (b). Conditions: Addition 1 is an aqueous solution of 30 μM sensor. Addition 2 has 20 mM Fe^{2+} or Co^{2+} solution added to the original solution. Addition 3 has had 2.3 μL of 20 mM EDTA added to it. Addition 4 has more Fe^{2+} or Co^{2+}, addition 5 has more EDTA, and addition 6 has more Fe^{2+} or Cu^{2+} again.

(a)

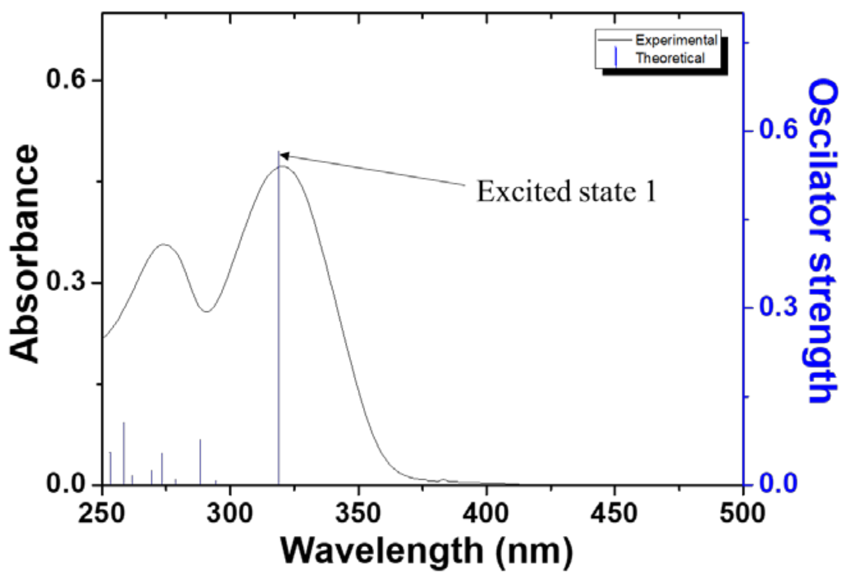

(b)

Excited state 1	Wavelength (nm)	Percent (%)	Main Character	Oscillator strength
H→L	318.98	93	$\pi \rightarrow \pi^*$	0.5675

Figure S11. (a) The theoretical excitation energies and the experimental UV-vis spectrum of sensor. (b) The major electronic transition energies and molecular orbital contributions of sensor (H = HOMO and L= LUMO)

(a)

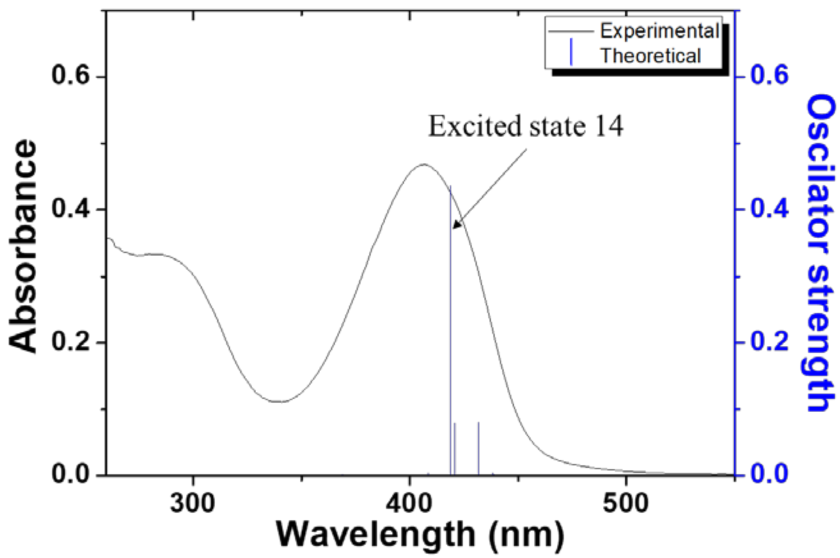

(b)

Excited state 14	Wavelength (nm)	Percent (%)	Main Character	Oscillator strength
H→L+1 (α)	418.81	23	ICT, LMCT	0.4367
H→L+2 (β)		41	ICT, LMCT	

Figure S12. (a) The theoretical excitation energies and the experimental UV-vis spectrum of Cu(II)-sensor complex. (b) The major electronic transition energies and molecular orbital contributions of Cu(II)-sensor complex (H = HOMO and L = LUMO).

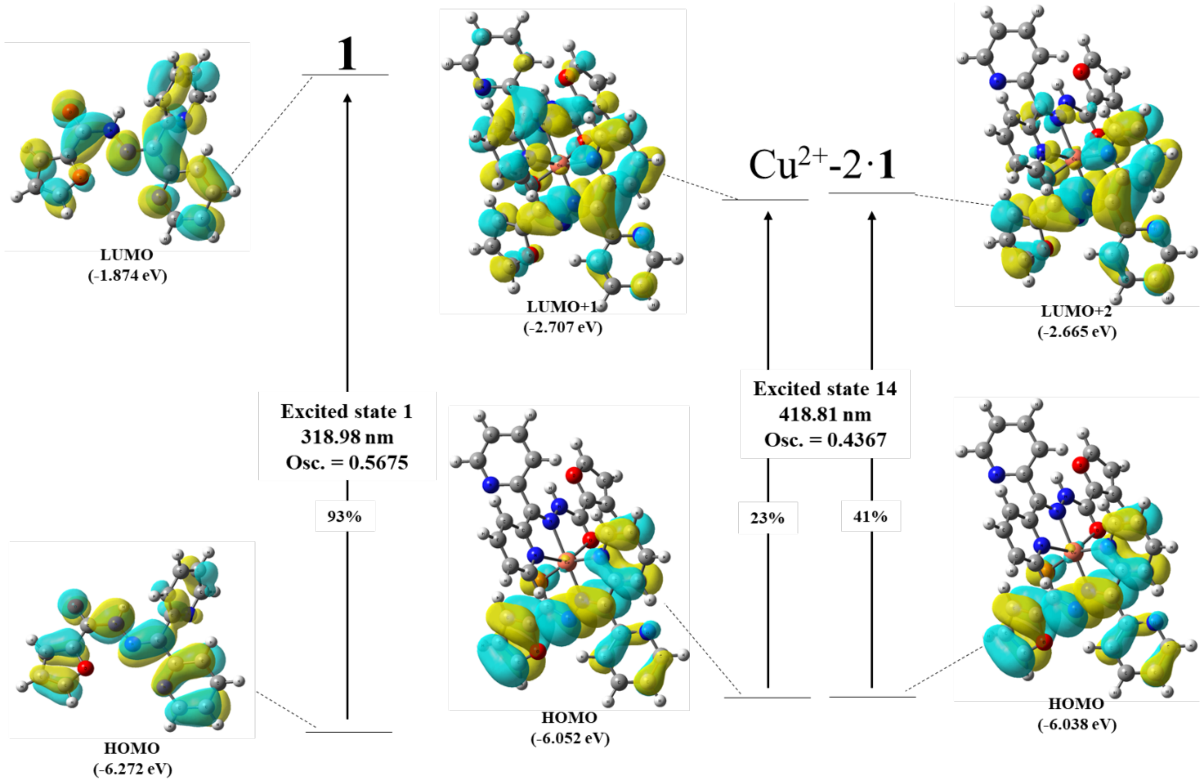

Figure S13. Molecular orbital diagrams of sensor and Cu(II)-sensor complex using TD-DFT.